Supplemental Document

Biomedical Optics EXPRESS

Towards label-free 3D segmentation of optical coherence tomography images of the optic nerve head using deep learning: supplement

SRIPAD KRISHNA DEVALLA,[1] TAN HUNG PHAM,[1,2] SATISH KUMAR PANDA,[1] LIANG ZHANG,[1] GIRIDHAR SUBRAMANIAN,[1] ANIRUDH SWAMINATHAN,[1] CHIN ZHI YUN,[1] MOHAN RAJAN,[3] SUJATHA MOHAN,[3] RAMASWAMI KRISHNADAS,[4] VIJAYALAKSHMI SENTHIL,[4] JOHN MARK S. DE LEON,[5] TIN A. TUN,[1,2] CHING-YU CHENG,[2,6] LEOPOLD SCHMETTERER,[2,7,9,10,11] SHAMIRA PERERA,[2,8] TIN AUNG,[2,8] ALEXANDRE H. THIÉRY,[12,14] AND MICHAËL J. A. GIRARD[13,15]

[1] *Ophthalmic Engineering & Innovation Laboratory, Department of Biomedical Engineering, Faculty of Engineering, National University of Singapore, Singapore*
[2] *Singapore Eye Research Institute, Singapore National Eye Centre, Singapore*
[3] *Rajan Eye Care Hospital, Chennai, India*
[4] *Glaucoma Services, Aravind Eye Care Systems, Madurai, India*
[5] *Department of Health Eye Center, East Avenue Medical Center, Quezon City, Philippines*
[6] *Ophthalmology & Visual Sciences Academic Clinical Program (Eye ACP), Duke-NUS Medical School, Singapore*
[7] *Nanyang Technological University, Singapore*
[8] *Duke-NUS Graduate Medical School, 8 College Rd, Singapore 169857, Singapore*
[9] *Department of Clinical Pharmacology, Medical University of Vienna, Austria*
[10] *Center for Medical Physics and Biomedical Engineering, Medical University of Vienna, Austria*
[11] *Institute of Clinical and Molecular Ophthalmology, Basel, Switzerland*
[12] *Department of Statistics and Applied Probability, National University of Singapore, Singapore*
[13] *Ophthalmic Engineering and Innovation Laboratory (OEIL), Singapore Eye Research Institute, 20 College Road, Singapore 169856, Singapore*
[14] *a.h.thiery@nus.edu.sg*
[15] *mgirard@ophthalmic.engineering*

Supplement DOI: https://doi.org/10.6084/m9.figshare.12857564

Parent Article DOI: https://doi.org/10.1364/BOE.395934

Supplement 1

Overall Schematic

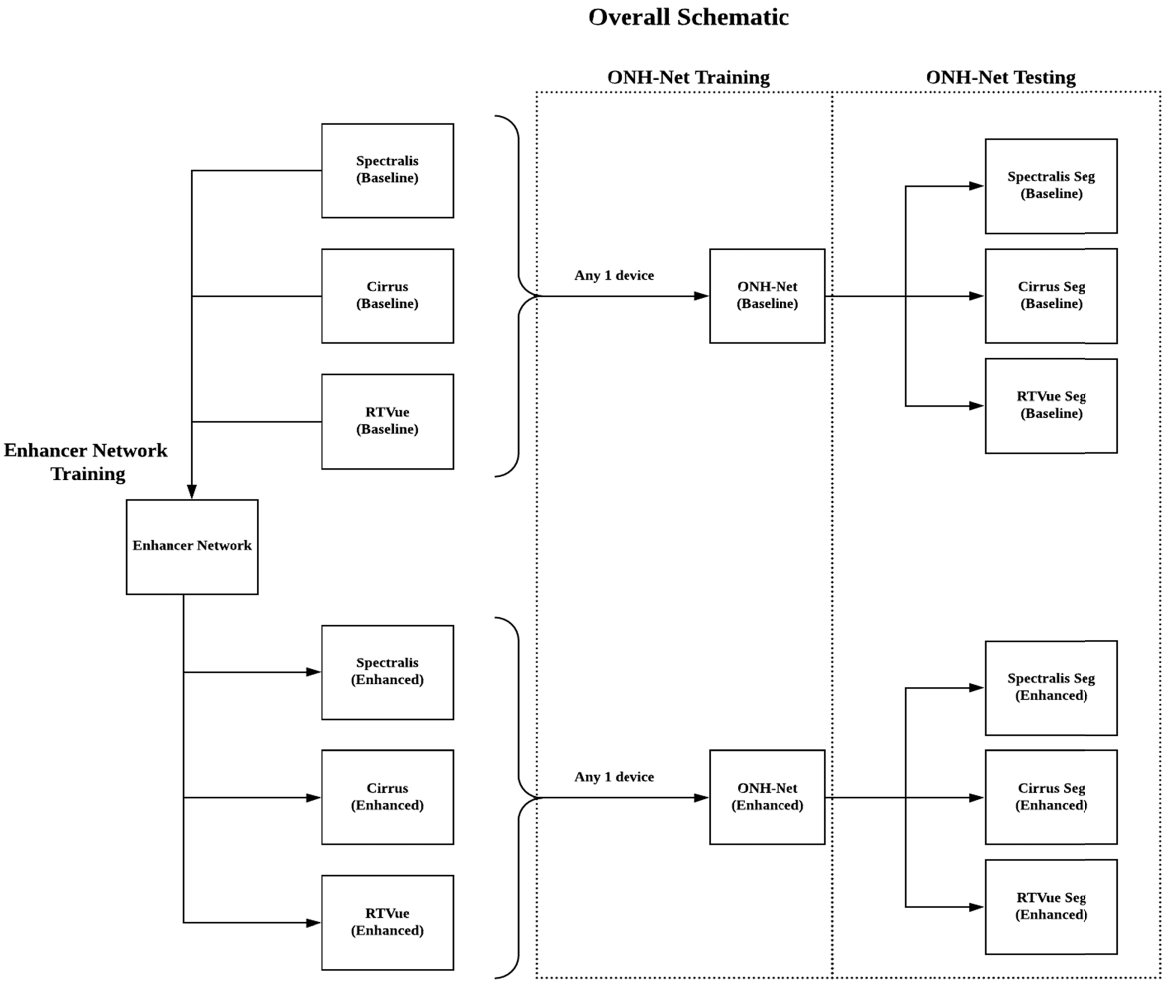

Fig. S1 : The overall schematic of the study is shown. Broadly, we developed two DL networks: the (1) enhancer network to enhance the OCT image quality from multiple devices; and (2) the ONH-Net to segment the individual ONH tissues from 3D OCT volumes.

Enhancer network – architecture

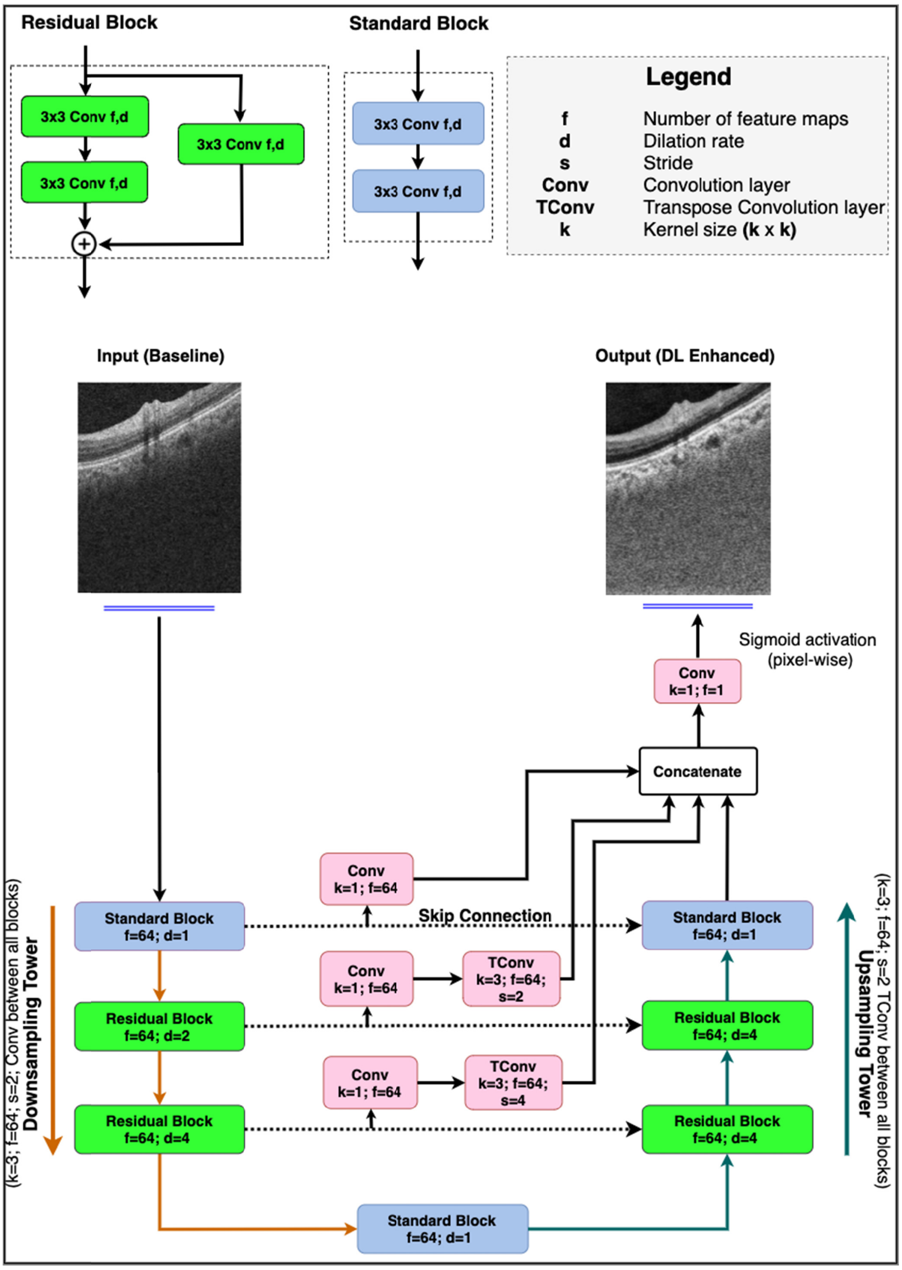

Fig. S2 : The enhancer network architecture is shown. Briefly, the network consisted of a downsampling tower to extract the contextual features (i.e., spatial arrangement of tissues) and an upsampling tower to extract the local features (i.e., tissue texture). The skip connections between the downsampling and upsampling towers helped to jointly learn the local and contextual information. Multiscale hierarchical feature extraction blocks (in pink) helped the network to obtain sharper tissue boundaries.

3D segmentation – network description

Segmentation CNN

Each of the three segmentation CNNs (**Fig. 2, A**) comprised of four micro-U-Nets (**Fig. 2, B; μ-U-Nets**), and a latent space (**Fig.2, C**).

In every segmentation CNN, each of the four μ-U-Nets repeatedly extracted the local (i.e., tissue texture), contextual (i.e., spatial arrangement of tissues), and depth-wise spatial (i.e., tissue morphology in 3D) information at multiple scales, with an aim to maximize the network's understanding of the ONH morphology with limited training data.

The segmentation CNNs and the μ-U-Nets followed the same style of design that was based on the U-Net architecture [58].

They consisted of an encoder segment that extracted contextual features (i.e. spatial arrangement of tissues), and a decoder segment that extracted the local information (i.e. tissue texture). The encoder segment sequentially downsampled the feature maps using the 3D max-pooling layers (stride=2,2,2), while the decoder segment sequentially upsampled using the 3D transposed convolutional layers (stride=2,2,2; filter size: 3x3x3; no of filters: 48).

The latent space, implemented using residual blocks similar to our earlier study [39], transferred the extracted features from the encoder to the decoder segment. The use of residual learning improved the flow of gradient information through the network.

Skip connections [40] between the encoder and decoder segments helped the DL network to jointly learn the contextual and local information, and the relationships between them.

Also, as implemented in our earlier study [39], we used multi-scale hierarchical feature extraction to improve the delineation of tissue boundaries. The feature maps obtained from multi-scale hierarchical feature extraction were then added with the output of the decoder segment.

The three segmentation CNNs deferred from each other only in the design of the 'feature extraction' (FE) units (**Fig. 2, D; Types 1-3**) that were used in the μ-U-Nets.

The μ-U-Net used the FE units to extract the local, contextual, and depth-wise spatial information. Even among expert observers, there exists a good amount of intra- and inter-observer variability in the delineations of ambiguous region such as the choroid-scleral interface and the posterior LC boundaries. To simulate a similar effect, we designed three types of FE units. Type 1 and Type 2 FE units (**Fig.2, D; Types 1-2**) differed from each other only by an additional elu activation [95] layer at the input to simulate the intra-observer variability (same learning approach, subtle variability due to additional activation). Type 3 FE unit however had a different design style, simulating the effect of inter-observer variabilities (greater variability due to different learning approaches) when compared to Type 1 or Type 2 FE units. The ensemble learning approach was then used to synergize the multiple equally plausible predictions in an attempt to reduce the error.

In both the Type 1 and Type 2 FE units, the input was passed through three parallel pathways: (1) the identity pathway; (2) the planar pathway; and (3) the volumetric pathway. The identity pathway implemented using a 1x1x1 3D convolutional layer allowed the unimpeded flow of gradient information throughout the network. In the planar pathway, the information from any two dimensions was extracted by the network at once (filter size: 3x3x1 [height x width]; 3x1x3 [height x depth]; 1x3x3 [width x depth]; 48 filters each). The volumetric pathway exploited the depth-wise spatially related and continuous information from all three dimensions at once (i.e., tissue morphology) using three 3D convolutional layers (filter size: 3x3x3; no of filters: 48). Finally, the feature maps from all the three pathways were added, batch normalized [96], and elu activated [95].

In the Type 3 FE (**Fig. 2, D**) unit, the input was elu activated and passed on to three sets of simple residual blocks with 48, 96, and 144 filters, respectively. In each residual block, one 3D convolutional layer (filter size: 3x3x3) extracted the features, while a 1x1x1 3D convolution layer was used as the identity connection [42]. The feature maps were then added, elu activated, and passed on to the next block. Finally, the feature maps were batch normalized and elu activated.

For all three segmentation CNNs, the pre-final output feature maps (decoder output + multi-scale hierarchical feature extraction) were passed through a 3D convolutional layer (filter size: 1x1x1; no of filters: 8 [number of classes; 6 tissues + noise + vitreous humor]) and softmax activated to obtain the tissue-wise probability for each pixel. For each pixel, the tissue class of the highest probability was then assigned. Each segmentation CNN was trained separately end-to-end with stochastic gradient descent (SGD; learning rate: 0.01; Nesterov momentum: 0.05 [80]) optimizer, and the Jaccard distance [26] as the loss function.

Ensembler

The ensembler (**Fig. 2, E**) was implemented using three sets of 3D convolutional layers (specifications for each set; filter size [no of filters]: 3x3x3 [48]; 3x3x3 [96]; 3x3x3 [192]). A dropout [79] of 50% was used between each set to reduce overfitting and improve the generalizability of the DL network. The feature maps were then passed through two dense layers of 64 and 8 units (number of classes) respectively, that were separated by a dropout layer (50%). Finally, a softmax activation was applied to obtain the pixel-wise predictions.

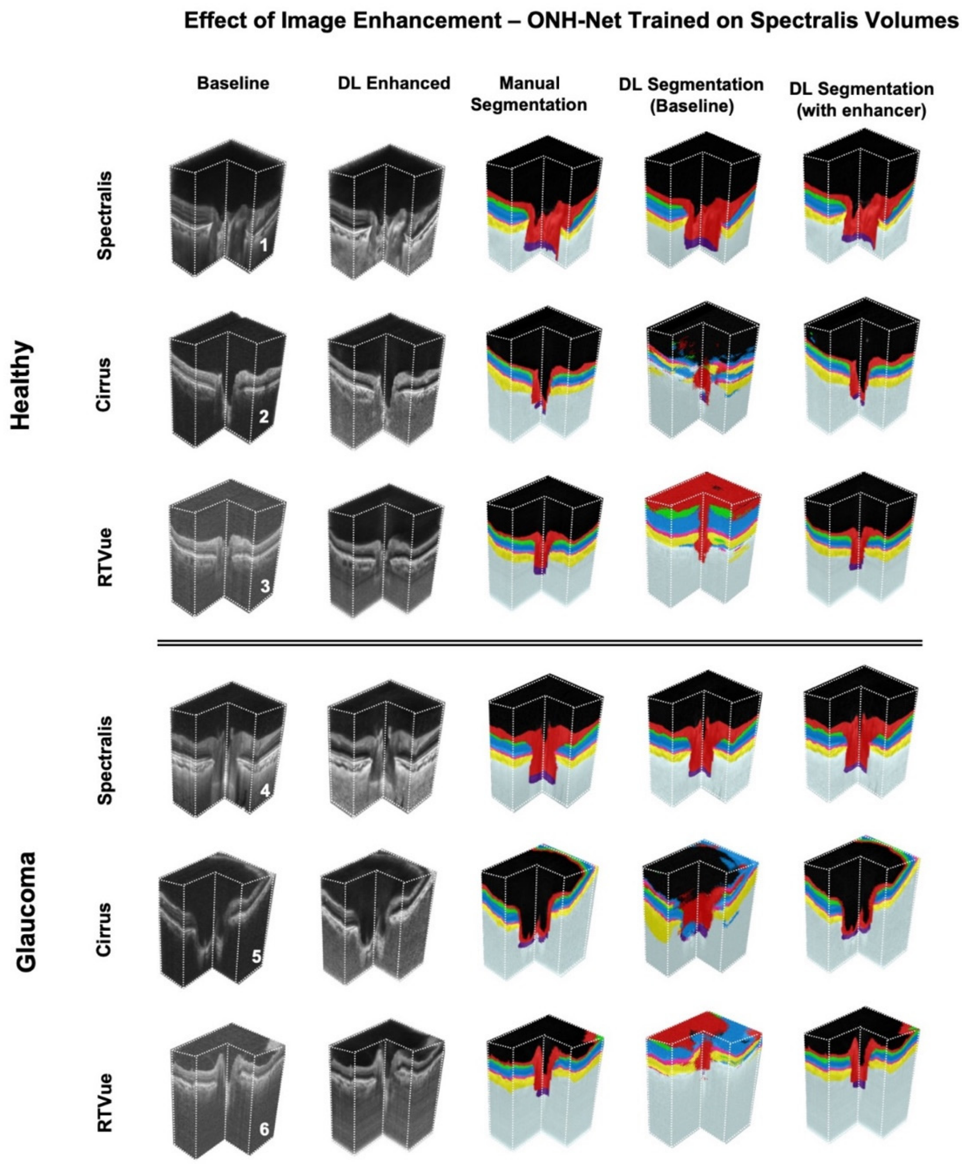

Fig. S3: The segmentation performance (in 3D) on three healthy (1-3) and three glaucoma (4-6) subjects is shown. The ONH-Net was trained on volumes from Spectralis, and tested on Spectralis (1, 4), Cirrus (2, 5), and RTVue (3, 6) devices respectively. The 1,st 2,nd and 3rd columns represent the baseline, DL enhanced, and the corresponding manual segmentations for the chosen volumes. The 4th and 5th columns represent the DL segmentations when the ONH-Net was trained with and without image enhancement respective.

3D segmentation clinical reliability – automated parameter extraction

Upon obtaining the DL segmentations, two clinically relevant structural parameters that are crucial for the diagnosis of glaucoma: the (1) peripapillary RNFL thickness (p-RNFLT); and the (2) peripapillary GCC thickness (p-GCCT) were automatically extracted as in our earlier works [26, 39].

For each volume in the testing dataset, a circular scan of diameter 3.4mm centered around the ONH [97] was obtained. The p-RNFL thickness (global) was computed as the distance between the inner limiting membrane and the posterior RNFL boundary (mean of 360° measure). The p-GCT (global) was computed as the distance between the posterior RNFL boundary and the inner plexiform layer boundary (mean of 360° measure).

The intraclass correlation coefficients (ICCs) were obtained to compare the measurements computed from the DL and their corresponding manual segmentations for all cases.

When trained and tested (same device) on the 'baseline' OCT volumes, the ICCs were always greater than 0.99 for both the p-RNFLT and the p-GCCT. However, when tested on the other two devices, since that the ONH-Net was unable to segment even a single tissue reliably, we did not extract the p-RNFLT and the g-GCCT for these cases.

When repeated the same with the 'DL-enhanced' volumes, irrespective of the device used for training, the ICCs were always greater than 0.98 for all cases, indicating excellent reliability.

We observed through our experiments that, irrespective of the device used for training, when tested on OCT volumes from a given device, the mean error (mean ± SD) in the measurement of the p-RNFLT was always less than 4.98 ± 1.3 µm, while for p-GCT, it was always less than 6.01 ± 0.9 µm. Although the preliminary results of device-independency seem encouraging, further validation and understanding is required by comparing clinically relevant measurements across DL models to truly assess its clinical value.

Benchmarking of the ONH-Net against 3D DRUNET

To better highlight the significance of the proposed 3D segmentation approach, the performance of the ONH-Net was compared against the 3D variant of our earlier DRUNET architecture [26] that offered an excellent performance in the segmentation of the individual ONH tissues (2D). We trained and tested (with DL enhanced images) the 3D variant of DRUNET by replacing the 2D layers (convolutional and pooling) with their 3D equivalent. Overall, for all cases, we observed that, the ONH-Net performed significantly superior than the 3D DRUNET. The performance (quantitative) comparison can be found in **Table S14**.

Table S1. The quantitative segmentation performance (**DC: Dice coefficient; Sn: sensitivity; Sp: specificity**) of ONH-Net with (**w**) and without (**w/o**) the use of image enhancement for glaucoma subjects. ONH-Net was trained on Spectralis, and tested on Spectralis, Cirrus, RTVue devices. The metrics for each tissue that were significantly higher (p<0.05) when image enhancement was used are underlined and in bold.

Effect of Image Enhancement - Spectralis Trained Framework (Glaucoma Subjects)											
Testing Device		**RNFL**		**GCC**		**Other Retinal Layers**		**RPE**		**Choroid**	
		w/o	**w**	**w/o**	**w**	**w/o**	**w**	**w/o**	**w**	**w/o**	**w**
Spectralis	**DC**	0.943±0.02	0.933±0.017	0.873±0.019	**0.931±0.032**	0.932±0.021	**0.951±0.031**	0.921±0.005	0.931±0.026	0.941±0.016	**0.934±0.012**
	Sn	0.928±0.011	**0.964±0.028**	0.921±0.048	0.933±0.002	0.955±0.041	**0.972±0.005**	0.927±0.025	0.955±0.001	0.933±0.036	0.942±0.001
	Sp	0.987±0.001	0.996±0.002	0.979±0.006	0.985±0.007	0.968±0.008	0.984±0.000	0.976±0.002	0.981±0.005	0.973±0.002	0.988±0.009
Cirrus	**DC**	0.500±0.049	**0.913±0.033**	0.332±0.052	**0.901±0.037**	0.617±0.040	**0.918±0.031**	0.562±0.020	**0.918±0.019**	0.477±0.055	**0.902±0.033**
	Sn	0.701±0.035	**0.955±0.024**	0.560±0.031	**0.909±0.014**	0.720±0.012	**0.901±0.018**	0.711±0.035	**0.925±0.016**	0.710±0.025	**0.913±0.041**
	Sp	0.803±0.021	**0.972±0.000**	0.723±0.014	**0.963±0.028**	0.865±0.012	**0.975±0.006**	0.813±0.016	**0.966±0.018**	0.832±0.035	**0.985±0.009**
RTVue	**DC**	0.364±0.004	**0.922±0.010**	0.266±0.019	**0.873±0.031**	0.308±0.025	**0.912±0.002**	0.311±0.036	**0.954±0.031**	0.302±0.041	**0.955±0.001**
	Sn	0.531±0.013	**0.914±0.022**	0.489±0.034	**0.959±0.021**	0.434±0.015	**0.928±0.022**	0.535±0.026	**0.962±0.025**	0.546±0.047	**0.942±0.025**
	Sp	0.622±0.009	**0.981±0.008**	0.536±0.008	**0.972±0.004**	0.577±0.016	**0.983±0.005**	0.706±0.011	**0.968±0.012**	0.762±0.025	**0.957±0.015**

Table S2. The quantitative segmentation performance (**DC: Dice coefficient; Sn: sensitivity; Sp: specificity**) of ONH-Net with (**w**) and without (**w/o**) the use of image enhancement for healthy subjects. ONH-Net was trained on Spectralis, and tested on Spectralis, Cirrus, RTVue devices. The metrics for each tissue that were significantly higher (p<0.05) when image enhancement was used are underlined and in bold.

Effect of Image Enhancement - Spectralis Trained Framework (Healthy Subjects)											
Testing Device		**RNFL**		**GCC**		**Other Retinal Layers**		**RPE**		**Choroid**	
		w/o	**w**	**w/o**	**w**	**w/o**	**w**	**w/o**	**w**	**w/o**	**w**
Spectralis	**DC**	0.959±0.001	0.965±0.004	0.913±0.023	**0.952±0.002**	0.892±0.013	0.911±0.023	0.871±0.002	**0.925±0.023**	0.863±0.032	0.918±0.013
	Sn	0.964±0.002	0.956±0.002	0.879±0.012	0.959±0.001	0.879±0.025	0.**922±0.018**	0.885±0.024	**0.921±0.031**	0.907±0.013	0.900±0.034
	Sp	0.976±0.005	0.989±0.000	0.984±0.004	0.988±0.001	0.982±0.000	0.985±0.001	0.974±0.021	0.984±0.011	0.956±0.021	0.988±0.001
Cirrus	**DC**	0.490±0.042	**0.965±0.011**	0.335±0.014	**0.873±0.032**	0.599±0.012	**0.904±0.031**	0.501±0.011	**0.894±0.021**	0.464±0.025	**0.873±0.041**
	Sn	0.713±0.022	**0.944±0.021**	0.585±0.025	**0.887±0.012**	0.716±0.015	**0.973±0.015**	0.655±0.025	**0.915±0.002**	0.664±0.016	**0.879±0.004**
	Sp	0.759±0.041	**0.935±0.018**	0.681±0.021	**0.966±0.001**	0.757±0.031	**0.954±0.005**	0.781±0.026	**0.982±0.003**	0.762±0.027	**0.997±0.001**
RTVue	**DC**	0.282±0.012	**0.923±0.004**	0.296±0.051	**0.923±0.021**	0.268±0.027	**0.885±0.025**	0.363±0.031	**0.873±0.013**	0.412±0.021	**0.913±0.024**
	Sn	0.503±0.025	**0.958±0.007**	0.441±0.021	**0.903±0.049**	0.498±0.022	**0.898±0.007**	0.515±0.002	**0.858±0.026**	0.488±0.008	**0.895±0.018**
	Sp	0.734±0.023	**0.986±0.003**	0.508±0.025	**0.988±0.004**	0.619±0.052	**0.977±0.001**	0.755±0.025	**0.984±0.004**	0.658±0.024	**0.983±0.004**

Table S3. The quantitative segmentation performance (**DC: Dice coefficient; Sn: sensitivity; Sp: specificity**) of the ONH-Net with (**w**) and without (**w/o**) the use of image enhancement for glaucoma subjects. The ONH-Net was trained on Cirrus, and tested on Spectralis, Cirrus, RTVue devices. The metrics for each tissue that were significantly higher (p<0.05) when image enhancement was used are underlined and in bold.

Effect of Image Enhancement - Cirrus Trained Framework (Glaucoma Subjects)											
Testing Device		**RNFL**		**GCC**		**Other Retinal Layers**		**RPE**		**Choroid**	
		w/o	**w**	**w/o**	**w**	**w/o**	**w**	**w/o**	**w**	**w/o**	**w**
Spectralis	**DC**	0.774±0.032	**0.951±0.002**	0.732±0.026	**0.964±0.005**	0.722±0.042	**0.941±0.011**	0.568±0.003	**0.912±0.004**	0.555±0.034	**0.941±0.023**
	Sn	0.789±0.02	**0.952±0.011**	0.821±0.033	**0.955±0.011**	0.841±0.023	**0.964±0.003**	0.799±0.025	**0.952±0.028**	0.732±0.051	**0.941±0.011**
	Sp	0.812±0.016	**0.993±0.005**	0.811±0.027	**0.997±0.002**	0.863±0.021	**0.996±0.000**	0.811±0.012	**0.985±0.005**	0.821±0.021	**0.991±0.004**
Cirrus	**DC**	0.923±0.003	0.941±0.021	0.862±0.011	**0.900±0.014**	0.922±0.029	0.931±0.021	0.852±0.016	**0.901±0.005**	0.905±0.003	0.931±0.025
	Sn	0.954±0.027	0.966±0.021	0.905±0.026	**0.932±0.011**	0.901±0.015	**0.930±0.015**	0.921±0.021	0.939±0.021	0.932±0.011	0.945±0.011
	Sp	0.981±0.005	0.994±0.002	0.994±0.001	0.998±0.001	0.997±0.002	0.978±0.004	0.995±0.003	0.978±0.003	0.981±0.004	0.986±0.003
RTVue	**DC**	0.632±0.041	**0.921±0.027**	0.581±0.024	**0.921±0.021**	0.566±0.008	**0.932±0.021**	0.622±0.002	**0.925±0.031**	0.521±0.021	**0.913±0.012**
	Sn	0.644±0.037	**0.923±0.021**	0.721±0.031	**0.927±0.031**	0.679±0.021	**0.936±0.008**	0.761±0.024	**0.935±0.003**	0.755±0.027	**0.931±0.017**
	Sp	0.721±0.026	**0.990±0.001**	0.718±0.027	**0.991±0.004**	0.751±0.012	**0.981±0.002**	0.744±0.041	**0.995±0.000**	0.821±0.031	**0.983±0.004**

Table S4. The quantitative segmentation performance (**DC: Dice coefficient; Sn: sensitivity; Sp: specificity**) of the ONH-Net with (**w**) and without (**w/o**) the use of image enhancement for healthy subjects. The ONH-Net was trained on Cirrus, and tested on Spectralis, Cirrus, RTVue devices. The metrics for each tissue that were significantly higher (p<0.05) when image enhancement was used are underlined and in bold.

Effect of Image Enhancement - Cirrus Trained Framework (Healthy Subjects)

Testing Device		RNFL		GCC		Other Retinal Layers		RPE		Choroid	
		w/o	w	w/o	w	w/o	w	w/o	w	w/o	w
Spectralis	DC	0.714±0.025	<u>**0.941±0.005**</u>	0.656±0.025	<u>**0.906±0.024**</u>	0.676±0.022	<u>**0.905±0.011**</u>	0.646±0.024	<u>**0.912±0.004**</u>	0.529±0.031	<u>**0.933±0.022**</u>
	Sn	0.693±0.032	<u>**0.923±0.035**</u>	0.759±0.031	<u>**0.913±0.036**</u>	0.787±0.016	<u>**0.934±0.021**</u>	0.701±0.004	<u>**0.912±0.024**</u>	0.814±0.025	<u>**0.939±0.018**</u>
	Sp	0.758±0.018	<u>**0.981±0.003**</u>	0.723±0.029	<u>**0.987±0.000**</u>	0.853±0.025	<u>**0.972±0.021**</u>	0.791±0.026	<u>**0.986±0.011**</u>	0.883±0.009	<u>**0.993±0.036**</u>
Cirrus	DC	0.901±0.022	<u>**0.939±0.012**</u>	0.818±0.018	0.884±0.022	0.876±0.035	0.907±0.028	0.874±0.031	0.915±0.024	0.889±0.012	0.907±0.005
	Sn	0.918±0.005	<u>**0.952±0.006**</u>	0.883±0.024	<u>**0.924±0.029**</u>	0.879±0.011	<u>**0.920±0.016**</u>	0.913±0.038	0.927±0.021	0.894±0.018	<u>**0.931±0.028**</u>
	Sp	0.971±0.021	0.992±0.001	0.974±0.025	0.993±0.001	0.985±0.028	0.992±0.003	0.987±0.002	0.984±0.009	0.978±0.011	0.991±0.000
RTVue	DC	0.654±0.031	<u>**0.930±0.018**</u>	0.501±0.41	<u>**0.903±0.025**</u>	0.51±0.041	<u>**0.902±0.025**</u>	0.668±0.039	<u>**0.910±0.023**</u>	0.465±0.024	<u>**0.907±0.028**</u>
	Sn	0.642±0.029	<u>**0.899±0.031**</u>	0.563±0.039	<u>**0.893±0.003**</u>	0.641±0.024	<u>**0.926±0.005**</u>	0.689±0.026	<u>**0.915±0.024**</u>	0.775±0.019	<u>**0.921±0.011**</u>
	Sp	0.679±0.031	<u>**0.968±0.020**</u>	0.618±0.024	<u>**0.991±0.005**</u>	0.665±0.022	<u>**0.985±0.016**</u>	0.818±0.013	<u>**0.988±0.003**</u>	0.791±0.031	<u>**0.991±0.004**</u>

Table S5. The quantitative segmentation performance (**DC: Dice coefficient; Sn: sensitivity; Sp: specificity**) of the ONH-Net with (**w**) and without (**w/o**) the use of image enhancement for glaucoma subjects. The ONH-Net was trained on RTVue, and tested on Spectralis, Cirrus, RTVue devices. The metrics for each tissue that were significantly higher (p<0.05) when image enhancement was used are underlined and in bold.

Effect of Image Enhancement - RTVue Trained Framework (Glaucoma Subjects)

Testing Device		RNFL		GCC		Other Retinal Layers		RPE		Choroid	
		w/o	w	w/o	w	w/o	w	w/o	w	w/o	w
Spectralis	DC	0.747±0.022	<u>**0.931±0.013**</u>	0.663±0.040	<u>**0.932±0.015**</u>	0.647±0.029	<u>**0.921±0.025**</u>	0.632±0.039	<u>**0.925±0.025**</u>	0.577±0.058	<u>**0.925±0.022**</u>
	Sn	0.697±0.004	<u>**0.924±0.010**</u>	0.692±0.035	<u>**0.922±0.028**</u>	0.723±0.045	<u>**0.934±0.035**</u>	0.653±0.026	<u>**0.947±0.001**</u>	0.711±0.050	<u>**0.924±0.029**</u>
	Sp	0.822±0.027	<u>**0.982±0.003**</u>	0.723±0.012	<u>**0.996±0.000**</u>	0.716±0.010	<u>**0.992±0.001**</u>	0.752±0.020	<u>**0.998±0.002**</u>	0.741±0.004	<u>**0.989±0.006**</u>
Cirrus	DC	0.689±0.031	<u>**0.923±0.009**</u>	0.699±0.041	<u>**0.925±0.020**</u>	0.611±0.035	<u>**0.917±0.031**</u>	0.612±0.045	<u>**0.931±0.019**</u>	0.512±0.021	<u>**0.918±0.031**</u>
	Sn	0.731±0.028	<u>**0.944±0.012**</u>	0.713±0.033	<u>**0.933±0.018**</u>	0.751±0.030	<u>**0.932±0.029**</u>	0.788±0.039	<u>**0.911±0.023**</u>	0.672±0.041	<u>**0.915±0.028**</u>
	Sp	0.762±0.021	<u>**0.988±0.017**</u>	0.758±0.010	<u>**0.996±0.000**</u>	0.712±0.009	<u>**0.991±0.005**</u>	0.812±0.005	<u>**0.988±0.006**</u>	0.734±0.005	<u>**0.990±0.002**</u>
RTVue	DC	0.951±0.005	0.946±0.018	0.902±0.022	0.921±0.020	0.901±0.019	<u>**0.941±0.005**</u>	0.822±0.035	0.927±0.020	0.934±0.020	0.932±0.025
	Sn	0.926±0.011	<u>**0.941±0.003**</u>	0.921±0.020	0.930±0.011	0.909±0.020	0.906±0.008	0.919±0.008	0.940±0.023	0.911±0.031	<u>**0.942±0.008**</u>
	Sp	0.960±0.018	0.991±0.001	0.981±0.008	0.994±0.005	0.977±0.005	0.993±0.000	0.992±0.003	0.997±0.000	0.991±0.001	0.994±0.001

Table S6. The quantitative segmentation performance (**DC: Dice coefficient; Sn: sensitivity; Sp: specificity**) of the ONH-Net with (**w**) and without (**w/o**) the use of image enhancement for healthy subjects. The ONH-Net was trained on RTVue, and tested on Spectralis, Cirrus, RTVue devices. The metrics for each tissue that were significantly higher (p<0.05) when image enhancement was used are underlined and in bold.

Effect of Image Enhancement - RTVue Trained Framework (Healthy Subjects)											
Testing Device		**RNFL**		**GCC**		**Other Retinal Layers**		**RPE**		**Choroid**	
		w/o	**w**	**w/o**	**w**	**w/o**	**w**	**w/o**	**w**	**w/o**	**w**
Spectralis	**DC**	0.697±0.024	**0.940±0.004**	0.649±0.032	**0.912±0.028**	0.687±0.030	**0.918±0.026**	0.620±0.039	**0.915±0.020**	0.565±0.058	**0.915± 0.021**
	Sn	0.737±0.016	**0.938±0.005**	0.672±0.033	**0.915±0.028**	0.760±0.040	**0.921±0.031**	0.620±0.038	**0.917±0.036**	0.710±0.044	**0.922± 0.033**
	Sp	0.782±0.007	**0.992±0.005**	0.722±0.005	**0.994±0.001**	0.709±0.005	**0.990±0.001**	0.706±0.004	**0.996±0.003**	0.732±0.005	**0.985± 0.006**
Cirrus	**DC**	0.715±0.021	**0.931±0.021**	0.699±0.040	**0.939±0.024**	0.600±0.035	**0.907±0.031**	0.595±0.045	**0.909±0.029**	0.499±0.054	**0.911± 0.027**
	Sn	0.713±0.041	**0.934±0.018**	0.720±0.032	**0.916±0.028**	0.744±0.035	**0.922±0.030**	0.765±0.041	**0.901±0.025**	0.667±0.043	**0.905± 0.025**
	Sp	0.748±0.003	**0.992±0.004**	0.790±0.008	**0.993±0.004**	0.690±0.008	**0.990±0.001**	0.799±0.007	**0.984±0.008**	0.750±0.005	**0.993± 0.002**
RTVue	**DC**	0.933±0.006	0.936±0.026	0.906±0.029	**0.911±0.017**	0.895±0.021	**0.932±0.010**	0.881±0.035	**0.917±0.018**	0.925±0.020	0.928± 0.022
	Sn	0.938±0.021	0.933±0.009	0.898±0.035	0.928±0.019	0.915±0.020	0.901±0.019	0.899±0.026	**0.929±0.024**	0.890±0.031	**0.924± 0.020**
	Sp	0.996±0.003	0.978±0.016	0.988±0.004	0.991±0.003	0.985±0.001	0.995±0.001	0.990±0.004	0.995±0.003	0.989±0.002	0.991± 0.006

Table S7. The device independent segmentation performance (**DC: Dice coefficient; Sn: sensitivity; Sp: specificity**) of the ONH-Net (using DL-enhanced dataset) for glaucoma subjects. The volumes from Spectralis device were tested on three segmentation models (Spectralis, Cirrus, and RTVue trained).

Tissue (Spectralis Volumes; Glaucoma Subjects)		**Training Device**		
		Spectralis	**Cirrus**	**RTVue**
RNFL	**DC**	0.933±0.017	0.951±0.002	0.931±0.013
	Sn	0.964±0.028	0.952±0.011	0.924±0.010
	Sp	0.996±0.002	0.993±0.005	0.982±0.003
GCC	**DC**	0.931±0.032	0.964±0.005	0.932±0.015
	Sn	0.933±0.002	0.955±0.011	0.922±0.028
	Sp	0.985±0.007	0.997±0.002	0.996±0.000
Other Retinal Layers	**DC**	0.951±0.031	0.941±0.011	0.921±0.025
	Sn	0.972±0.005	0.964±0.003	0.934±0.035
	Sp	0.984±0.000	0.996±0.000	0.992±0.001
RPE	**DC**	0.931±0.026	0.912±0.004	0.925±0.025
	Sn	0.955±0.001	0.952±0.028	0.947±0.001
	Sp	0.981±0.005	0.985±0.005	0.998±0.002
Choroid	**DC**	0.934±0.012	0.941±0.023	0.925±0.022
	Sn	0.942±0.001	0.941±0.011	0.924±0.029
	Sp	0.988±0.009	0.991±0.004	0.989±0.006

Table S8. The device independent segmentation performance (**DC: Dice coefficient; Sn: sensitivity; Sp: specificity**) of the ONH-Net (using DL-enhanced dataset) for healthy subjects. The volumes from Spectralis device were tested on three segmentation models (Spectralis, Cirrus, and RTVue trained).

Tissue (Spectralis Volumes; Healthy Subjects)		**Training Device**		
		Spectralis	**Cirrus**	**RTVue**
RNFL	**DC**	0.965±0.004	0.941±0.005	0.940±0.004
	Sn	0.956±0.002	0.923±0.035	0.938±0.005
	Sp	0.989±0.000	0.981±0.003	0.992±0.005
GCC	**DC**	0.952±0.002	0.906±0.024	0.912±0.028
	Sn	0.959±0.001	0.913±0.036	0.915±0.028
	Sp	0.988±0.001	0.987±0.000	0.994±0.001
Other Retinal Layers	**DC**	0.911±0.023	0.905±0.011	0.918±0.026
	Sn	0.922±0.018	0.934±0.021	0.921±0.031
	Sp	0.985±0.001	0.972±0.021	0.990±0.001
RPE	**DC**	0.925±0.023	0.912±0.004	0.915±0.020
	Sn	0.921±0.031	0.912±0.024	0.917±0.036
	Sp	0.984±0.011	0.986±0.011	0.996±0.003
Choroid	**DC**	0.918±0.013	0.933±0.022	0.915± 0.021
	Sn	0.900±0.034	0.939±0.018	0.922± 0.033
	Sp	0.988±0.001	0.993±0.036	0.985± 0.006

Table S9. The device independent segmentation performance (**DC: Dice coefficient; Sn: sensitivity; Sp: specificity**) of the ONH-Net (using DL-enhanced dataset) for glaucoma subjects. The volumes from Cirrus device were tested on three segmentation models (Spectralis, Cirrus, and RTVue trained).

Tissue (Cirrus Volumes; Glaucoma Subjects)		Training Device		
		Spectralis	**Cirrus**	**RTVue**
RNFL	**DC**	0.913±0.033	0.941±0.021	0.923±0.009
	Sn	0.955±0.024	0.966±0.021	0.944±0.012
	Sp	0.972±0.000	0.994±0.002	0.988±0.017
GCC	**DC**	0.901±0.037	0.900±0.014	0.925±0.020
	Sn	0.909±0.014	0.932±0.011	0.933±0.018
	Sp	0.963±0.028	0.998±0.001	0.996±0.000
Other Retinal Layers	**DC**	0.918±0.031	0.931±0.021	0.917±0.031
	Sn	0.901±0.018	0.930±0.015	0.932±0.029
	Sp	0.975±0.006	0.978±0.004	0.991±0.005
RPE	**DC**	0.918±0.019	0.901±0.005	0.931±0.019
	Sn	0.925±0.016	0.939±0.021	0.911±0.023
	Sp	0.966±0.018	0.978±0.003	0.988±0.006
Choroid	**DC**	0.902±0.033	0.931±0.025	0.918±0.031
	Sn	0.913±0.041	0.945±0.011	0.915±0.028
	Sp	0.985±0.009	0.986±0.003	0.990±0.002

Table S10. The device independent segmentation performance (**DC: Dice coefficient; Sn: sensitivity; Sp: specificity**) of the ONH-Net (using DL-enhanced dataset) for healthy subjects. The volumes from Cirrus device were tested on three segmentation models (Spectralis, Cirrus, and RTVue trained).

Tissue (Cirrus Volumes; Healthy Subjects)		Training Device		
		Spectralis	**Cirrus**	**RTVue**
RNFL	**DC**	0.965±0.011	0.939±0.012	0.931±0.021
	Sn	0.944±0.021	0.952±0.006	0.934±0.018
	Sp	0.935±0.018	0.992±0.001	0.992±0.004
GCC	**DC**	0.873±0.032	0.884±0.022	0.939±0.024
	Sn	0.887±0.012	0.924±0.029	0.916±0.028
	Sp	0.966±0.001	0.993±0.001	0.993±0.004
Other Retinal Layers	**DC**	0.904±0.031	0.907±0.028	0.907±0.031
	Sn	0.973±0.015	0.920±0.016	0.922±0.030
	Sp	0.954±0.005	0.992±0.003	0.990±0.001
RPE	**DC**	0.894±0.021	0.915±0.024	0.909±0.029
	Sn	0.915±0.002	0.927±0.021	0.901±0.025
	Sp	0.982±0.003	0.984±0.009	0.984±0.008
Choroid	**DC**	0.873±0.041	0.907±0.005	0.911± 0.027
	Sn	0.879±0.004	0.931±0.028	0.905± 0.025
	Sp	0.997±0.001	0.991±0.000	0.993± 0.002

Table S11. The device independent segmentation performance (**DC: Dice coefficient; Sn: sensitivity; Sp: specificity**) of the ONH-Net (using DL-enhanced dataset) for glaucoma subjects. The volumes from RTVue device were tested on three segmentation models (Spectralis, Cirrus, and RTVue trained).

Tissue (RTVue Volumes; Glaucoma Subjects)		Training Device		
		Spectralis	**Cirrus**	**RTVue**
RNFL	**DC**	0.922±0.010	0.921±0.027	0.946±0.018
	Sn	0.914±0.022	0.923±0.021	0.941±0.003
	Sp	0.981±0.008	0.990±0.001	0.991±0.001
GCC	**DC**	0.873±0.031	0.921±0.021	0.921±0.020
	Sn	0.959±0.021	0.927±0.031	0.930±0.011
	Sp	0.972±0.004	0.991±0.004	0.994±0.005
Other Retinal Layers	**DC**	0.912±0.002	0.932±0.021	0.941±0.005
	Sn	0.928±0.022	0.936±0.008	0.906±0.008
	Sp	0.983±0.005	0.981±0.002	0.993±0.000
RPE	**DC**	0.954±0.031	0.925±0.031	0.927±0.020
	Sn	0.962±0.025	0.935±0.003	0.940±0.023
	Sp	0.968±0.012	0.995±0.000	0.997±0.000
Choroid	**DC**	0.955±0.001	0.913±0.012	0.932±0.025
	Sn	0.942±0.025	0.931±0.017	0.942±0.008
	Sp	0.957±0.015	0.983±0.004	0.994±0.001

Table S12. The device independent segmentation performance (**DC: Dice coefficient; Sn: sensitivity; Sp: specificity**) of the ONH-Net (using DL-enhanced dataset) for healthy subjects. The volumes from RTVue device were tested on three segmentation models (Spectralis, Cirrus, and RTVue trained).

Tissue (RTVue Volumes; Healthy Subjects)		Training Device		
		Spectralis	**Cirrus**	**RTVue**
RNFL	**DC**	0.923±0.004	0.930±0.018	0.936±0.026
	Sn	0.958±0.007	0.899±0.031	0.933±0.009
	Sp	0.986±0.003	0.968±0.020	0.978±0.016
GCC	**DC**	0.923±0.021	0.903±0.025	0.911±0.017
	Sn	0.903±0.049	0.893±0.003	0.928±0.019
	Sp	0.988±0.004	0.991±0.005	0.991±0.003
Other Retinal Layers	**DC**	0.885±0.025	0.902±0.025	0.932±0.010
	Sn	0.898±0.007	0.926±0.005	0.901±0.019
	Sp	0.977±0.001	0.985±0.016	0.995±0.001
RPE	**DC**	0.873±0.013	0.910±0.023	0.917±0.018
	Sn	0.858±0.026	0.915±0.024	0.929±0.024
	Sp	0.984±0.004	0.988±0.003	0.995±0.003
Choroid	**DC**	0.913±0.024	0.907±0.028	0.928± 0.022
	Sn	0.895±0.018	0.921±0.011	0.924± 0.020
	Sp	0.983±0.004	0.991±0.004	0.991± 0.006

Table S13: The quantitative segmentation performance (**DC: Dice coefficient; Sn: sensitivity; Sp: specificity**) of ONH-Net when trained and tested on the digitally enhanced (**Digital**) and the DL enhanced (**DL**) OCT volumes. The metrics for each tissue that were significantly higher (p<0.05) when the DL enhanced OCT volumes were used are underlined and in bold.

Comparison Between Digitally Enhanced and DL Enhanced Segmentations - Spectralis Trained Framework											
Testing Device		**RNFL**		**GCC**		**Other Retinal Layers**		**RPE**		**Choroid**	
		Digital	**DL**	**Digital**	**DL**	**Digital**	**DL**	**Digital**	**DL**	**Digital**	**DL**
Spectralis	**DC**	0.901±0.020	**0.954±0.017**	0.891±0.012	**0.931±0.020**	0.903±0.018	**0.936±0.010**	0.883±0.041	**0.918±0.014**	0.901±0.022	0.926± 0.031
	Sn	0.956±0.019	0.960±0.026	0.911 ±0.008	**0.946±0.019**	0.931±0.021	0.947±0.010	0.915±0.020	**0.938±0.022**	0.921±0.020	0.931± 0.038
	Sp	0.989±0.001	0.993±0.001	0.990±0.007	0.996±0.003	0.978±0.001	0.995±0.001	0.975±0.010	0.994±0.002	0.979±0.001	0.996± 0.002
Cirrus	**DC**	0.802±0.048	**0.943±0.027**	0.781±0.044	**0.919±0.032**	0.858±0.024	**0.918±0.031**	0.741±0.021	**0.918±0.019**	0.820±0.039	**0.902± 0.033**
	Sn	0.880±0.018	**0.955±0.024**	0.854±0.024	**0.899±0.024**	0.890±0.010	**0.937±0.020**	0.830±0.048	**0.920±0.023**	0.901±0.001	**0.896± 0.043**
	Sp	0.942±0.011	**0.988±0.000**	0.955±0.019	**0.983±0.004**	0.948±0.011	**0.992±0.004**	0.921±0.020	**0.991±0.001**	0.950±0.019	**0.991± 0.004**
RTVue	**DC**	0.778±0.039	**0.951±0.031**	0.721±0.056	**0.898±0.030**	0.801±0.038	**0.896±0.041**	0.691±0.056	**0.912±0.029**	0.783±0.042	**0.934± 0.028**
	Sn	0.858±0.023	**0.936±0.032**	0.860±0.044	**0.931±0.038**	0.901±0.031	**0.913±0.038**	0.780±0.051	**0.910±0.031**	0.872±0.033	**0.901± 0.028**
	Sp	0.902±0.020	**0.996±0.003**	0.910±0.013	**0.992±0.006**	0.930±0.009	**0.994±0.005**	0.840±0.039	**0.994±0.003**	0.903±0.026	**0.994± 0.005**

Comparison Between Digitally Enhanced and DL Enhanced Segmentations - Cirrus Trained Framework											
Testing Device		**RNFL**		**GCC**		**Other Retinal Layers**		**RPE**		**Choroid**	
		Digital	**DL**	**Digital**	**DL**	**Digital**	**DL**	**Digital**	**DL**	**Digital**	**DL**
Spectralis	**DC**	0.689±0.033	**0.966±0.027**	0.654±0.045	**0.935±0.020**	0.760±0.039	**0.923±0.023**	0.701±0.038	**0.932±0.018**	0.662±0.041	**0.937± 0.029**
	Sn	0.734±0.037	**0.946±0.031**	0.790±0.022	**0.934±0.021**	0.834±0.033	**0.949±0.027**	0.770±0.044	**0.932±0.032**	0.760±0.037	**0.940± 0.034**
	Sp	0.801±0.004	**0.987±0.000**	0.767±0.036	**0.992±0.002**	0.878±0.003	**0.994±0.002**	0.811±0.003	**0.995±0.003**	0.829±0.020	**0.995± 0.002**
Cirrus	**DC**	0.924±0.019	**0.965±0.022**	0.880±0.034	**0.920±0.027**	0.891±0.018	**0.932±0.026**	0.848±0.041	**0.913±0.020**	0.871±0.024	**0.924± 0.025**
	Sn	0.966±0.031	0.974±0.030	0.899±0.028	0.918±0.026	0.920±0.020	0.922±0.021	0.907±0.026	**0.933±0.015**	0.913±0.033	0.923± 0.028
	Sp	0.969±0.002	**0.988±0.001**	0.984±0.002	0.994±0.002	0.991±0.004	0.995±0.001	0.991±0.002	0.996±0.002	0.989±0.001	0.993± 0.005
RTVue	**DC**	0.761±0.049	**0.936±0.035**	0.701±0.025	**0.896±0.029**	0.794±0.059	**0.917±0.028**	0.699±0.045	**0.905±0.030**	0.712±0.054	**0.910± 0.031**
	Sn	0.801±0.028	**0.925±0.033**	0.820±0.039	**0.920±0.031**	0.860±0.048	**0.928±0.022**	0.760±0.038	**0.925±0.027**	0.765±0.055	**0.926± 0.034**
	Sp	0.867±0.010	**0.980±0.003**	0.880±0.018	**0.986±0.004**	0.908±0.010	**0.988±0.003**	0.831±0.020	**0.990±0.004**	0.816±0.010	**0.990± 0.005**

Comparison Between Digitally Enhanced and DL Enhanced Segmentations - RTVue Trained Framework											
Testing Device		**RNFL**		**GCC**		**Other Retinal Layers**		**RPE**		**Choroid**	
		Digital	**DL**	**Digital**	**DL**	**Digital**	**DL**	**Digital**	**DL**	**Digital**	**DL**
Spectralis	**DC**	0.701±0.028	**0.966±0.029**	0.646±0.032	**0.912±0.028**	0.721±0.043	**0.918±0.026**	0.667±0.033	**0.915±0.020**	0.701±0.036	**0.915± 0.021**
	Sn	0.768±0.017	**0.951±0.035**	0.766±0.039	**0.915±0.028**	0.831±0.036	**0.931±0.031**	0.730±0.028	**0.917±0.036**	0.770±0.044	**0.922± 0.033**
	Sp	0.830±0.018	**0.986±0.003**	0.804±0.012	**0.994±0.003**	0.870±0.016	**0.996±0.001**	0.808±0.010	**0.996±0.003**	0.822±0.025	**0.985± 0.006**
Cirrus	**DC**	0.728±0.026	**0.942±0.024**	0.662±0.041	**0.939±0.024**	0.701±0.033	**0.907±0.031**	0.630±0.042	**0.909±0.029**	0.711±0.036	**0.911± 0.027**
	Sn	0.770±0.033	**0.954±0.033**	0.720±0.038	**0.916±0.028**	0.784±0.029	**0.922±0.030**	0.705±0.034	**0.901±0.035**	0.778±0.026	**0.905± 0.025**
	Sp	0.822±0.021	**0.995±0.002**	0.799±0.020	**0.993±0.004**	0.848±0.020	**0.994±0.002**	0.769±0.010	**0.984±0.008**	0.799±0.018	**0.993± 0.002**
RTVue	**DC**	0.902±0.028	**0.951±0.028**	0.900±0.019	0.911±0.017	0.915±0.021	0.925±0.008	0.878±0.025	**0.917±0.018**	0.919±0.020	0.931± 0.022
	Sn	0.920±0.020	**0.947±0.010**	0.918±0.025	0.928±0.019	0.922±0.020	0.931±0.019	0.901±0.026	**0.929±0.024**	0.921±0.030	0.924± 0.020
	Sp	0.980±0.009	**0.997±0.001**	0.987±0.005	0.991±0.003	0.965±0.001	**0.995±0.001**	0.990±0.004	0.995±0.003	0.989±0.002	0.991± 0.006

Table S14: The quantitative segmentation performance (**DC: Dice coefficient; Sn: sensitivity; Sp: specificity**) comparison between the 3D DRUNET and the ONH-Net when trained and tested on the DL enhanced OCT volumes. The metrics for each tissue that were significantly higher (p<0.05) are underlined and in bold.

Performance Comparison Between DRUNET and ONH-Net - Spectralis Trained Framework

Testing Device		RNFL		GCC		Other Retinal Layers		RPE		Choroid	
		DRUNET	ONH-Net	DRUNET	ONH-Net	DRUNET	ONH-Net	DRUNET	ONH-Net	DRUNET	ONH-Net
Spectralis	DC	0.845±0.018	**0.954±0.017**	0.820±0.015	**0.931±0.020**	0.860±0.011	**0.936±0.010**	0.790±0.041	**0.918±0.014**	0.868±0.012	**0.926± 0.031**
	Sn	0.923±0.016	**0.960±0.026**	0.920 ±0.008	**0.946±0.019**	0.941±0.021	**0.947±0.010**	0.915±0.020	**0.938±0.022**	0.921±0.020	**0.931± 0.038**
	Sp	0.978±0.004	**0.993±0.001**	0.969±0.011	**0.996±0.003**	0.981±0.001	0.995±0.001	0.956±0.009	**0.994±0.002**	0.983±0.001	0.996± 0.002
Cirrus	DC	0.748±0.024	**0.943±0.027**	0.702±0.014	**0.919±0.032**	0.763±0.033	**0.918±0.031**	0.699±0.022	**0.918±0.019**	0.734±0.032	**0.902± 0.033**
	Sn	0.852±0.021	**0.955±0.024**	0.824±0.024	**0.899±0.024**	0.870±0.012	**0.937±0.020**	0.801±0.032	**0.920±0.023**	0.846±0.020	**0.896± 0.043**
	Sp	0.899±0.014	**0.988±0.000**	0.867±0.019	**0.983±0.004**	0.901±0.010	**0.992±0.004**	0.813±0.022	**0.991±0.001**	0.899±0.021	**0.991± 0.004**
RTVue	DC	0.721±0.023	**0.951±0.031**	0.701±0.036	**0.898±0.030**	0.753±0.030	**0.896±0.041**	0.676±0.048	**0.912±0.029**	0.756±0.038	**0.934± 0.028**
	Sn	0.832±0.023	**0.936±0.032**	0.810±0.031	**0.931±0.038**	0.867±0.028	**0.913±0.038**	0.750±0.041	**0.910±0.031**	0.851±0.030	**0.901± 0.028**
	Sp	0.870±0.020	**0.996±0.003**	0.850±0.020	**0.992±0.006**	0.899±0.012	**0.994±0.005**	0.811±0.021	**0.994±0.003**	0.880±0.022	**0.994± 0.005**

Performance Comparison Between DRUNET and ONH-Net - Cirrus Trained Framework

Testing Device		RNFL		GCC		Other Retinal Layers		RPE		Choroid	
		DRUNET	ONH-Net	DRUNET	ONH-Net	Digitally En	DL En	DRUNET	ONH-Net	DRUNET	ONH-Net
Spectralis	DC	0.701 ±0.023	**0.966±0.027**	0.661±0.032	**0.935±0.020**	0.743±0.039	**0.923±0.023**	0.676±0.028	**0.932±0.018**	0.712±0.036	**0.937± 0.029**
	Sn	0.791±0.026	**0.946±0.031**	0.743±0.021	**0.934±0.021**	0.823±0.030	**0.949±0.027**	0.750±0.024	**0.932±0.032**	0.789±0.031	**0.940± 0.034**
	Sp	0.810±0.021	**0.987±0.000**	0.801±0.026	**0.992±0.002**	0.889±0.012	**0.994±0.002**	0.791±0.013	**0.995±0.003**	0.803±0.021	**0.995± 0.002**
Cirrus	DC	0.856±0.016	**0.965±0.022**	0.803±0.042	**0.920±0.027**	0.889±0.021	**0.932±0.026**	0.800±0.032	**0.913±0.020**	0.876±0.014	**0.924± 0.025**
	Sn	0.920±0.024	**0.974±0.030**	0.887±0.025	**0.918±0.026**	0.920±0.020	0.922±0.021	0.880±0.022	**0.933±0.015**	0.922±0.030	0.923± 0.028
	Sp	0.956±0.010	**0.988±0.001**	0.941±0.012	**0.994±0.002**	0.967±0.009	**0.995±0.001**	0.942±0.014	**0.996±0.002**	0.978±0.021	**0.993± 0.005**
RTVue	DC	0.743±0.038	**0.936±0.035**	0.699±0.022	**0.896±0.029**	0.767±0.045	**0.917±0.028**	0.702±0.042	**0.905±0.030**	0.756±0.045	**0.910± 0.031**
	Sn	0.834±0.011	**0.925±0.033**	0.760±0.032	**0.920±0.031**	0.856±0.032	**0.928±0.022**	0.789±0.034	**0.925±0.027**	0.823±0.050	**0.926± 0.034**
	Sp	0.889±0.009	**0.980±0.003**	0.834±0.017	**0.986±0.004**	0.881±0.009	**0.988±0.003**	0.821±0.022	**0.990±0.004**	0.856±0.013	**0.990± 0.005**

Performance Comparison Between DRUNET and ONH-Net - RTVue Trained Framework

Testing Device		RNFL		GCC		Other Retinal Layers		RPE		Choroid	
		DRUNET	ONH-Net	DRUNET	ONH-Net	DRUNET	ONH-Net	DRUNET	ONH-Net	DRUNET	ONH-Net
Spectralis	DC	0.711±0.023	**0.966±0.029**	0.700±0.034	**0.912±0.028**	0.733±0.021	**0.918±0.026**	0.676±0.020	**0.915±0.020**	0.733±0.022	**0.915± 0.021**
	Sn	0.801±0.012	**0.951±0.035**	0.778±0.031	**0.915±0.028**	0.846±0.020	**0.931±0.031**	0.765±0.022	**0.917±0.036**	0.820±0.037	**0.922± 0.033**
	Sp	0.823±0.014	**0.986±0.003**	0.802±0.022	**0.994±0.003**	0.851±0.010	**0.996±0.001**	0.787±0.010	**0.996±0.003**	0.855±0.030	**0.985± 0.006**
Cirrus	DC	0.699±0.021	**0.942±0.024**	0.689±0.032	**0.939±0.024**	0.711±0.032	**0.907±0.031**	0.661±0.052	**0.909±0.029**	0.710±0.030	**0.911± 0.027**
	Sn	0.750±0.032	**0.954±0.033**	0.750±0.025	**0.916±0.028**	0.794±0.022	**0.922±0.030**	0.755±0.041	**0.901±0.035**	0.788±0.022	**0.905± 0.025**
	Sp	0.792±0.040	**0.995±0.002**	0.769±0.025	**0.993±0.004**	0.800±0.014	**0.994±0.002**	0.770±0.021	**0.984±0.008**	0.801±0.008	**0.993± 0.002**
RTVue	DC	0.780±0.012	**0.951±0.028**	0.732±0.034	**0.911±0.017**	0.790±0.023	**0.925±0.008**	0.765±0.024	**0.917±0.018**	0.775±0.026	**0.931± 0.022**
	Sn	0.856±0.011	**0.947±0.010**	0.812±0.023	**0.928±0.019**	0.856±0.024	**0.931±0.019**	0.845±0.015	**0.929±0.024**	0.867±0.042	**0.924± 0.020**
	Sp	0.880±0.009	**0.997±0.001**	0.833±0.010	**0.991±0.003**	0.899±0.008	**0.995±0.001**	0.867±0.008	**0.995±0.003**	0.899±0.032	**0.991± 0.006**